

COMPUTATION OF FAST ION CONFINEMENT BY ELECTRIC FIELDS  
IN THE W VII A STELLARATOR

F.P. Penningsfeld, W. Ott and E. Speth

Max-Planck-Institut für Plasmaphysik  
EURATOM-Association, D-8046 Garching

**Abstract:** The confinement of fast injected ions in W VII-A is strongly affected by the presence of radial electric fields. The neutral beam deposition code ODIN so far had been valid for the treatment of small electric fields ( $|E| \leq 100$  V/cm) and therefore had to be revised to cover large electric fields as well. The accuracy achieved for typical cases has been estimated by using a perturbation method.

It is shown that the new version of ODIN gives correct results within an error of  $\pm 10\%$  for the total heating efficiency and  $\pm 20\%$  for the power deposition profiles up to 5.0 kV radial electric potential. The observed heating efficiency for co and counter injection  $\eta \approx 0.35$  is very well represented by code results for a potential of 2.0 kV with negligible influence of its radial dependence.

**Introduction:** At the beginning of NBI experiments on W VII-A a heating efficiency was found experimentally that was higher than predicted by the numerical simulations /1/. An explanation of this fact was the occurrence of a radial electric field confirmed by the observation of a fast poloidal plasma rotation /2/ which was not considered in the numerical calculations. The beneficial effect of an electric field on  $\eta$  was then confirmed qualitatively by ODIN calculations /3/. However, for large electric fields the quantitative results showed a number of inconsistencies, which required a revision of the code. The subsequent improvements and an investigation of the resulting accuracy are described in the first part of this paper. In the second part the new version is used to recalculate the heating efficiency for W VII-A and to demonstrate the influence of the electric field on the orbit of single particles. The results are in qualitative accordance with a bounce averaged Monte-Carlo simulation /4/.

I. Revision of the neutral beam heating code ODIN:

The improvements that become necessary in order to include large electric fields are: energy conservation, time step control and a more careful modelling of the electric field.

**I.1 Energy conservation:** For a correct energy balance for each injected particle in the presence of electric fields the potential energy  $q_b \cdot \varphi$  of an ion at every point of the trajectory has to be calculated to conserve the total energy

$$E_{\text{tot}} = 1/2 m_b v_b^2 + q_b \varphi(r) = \text{const.}$$

The term  $q_b \varphi$  previously not included may be neglected only for  $q_b \varphi \ll E_b$ .

**I.2 Timestep control:** The ExB-drift causes an additional poloidal velocity exceeding the  $\nabla B$  and curvature drift of the fast ions for  $|E| > 135$  V/cm at W VII-A conditions. The dynamic adaptation of the iteration time step of

the orbit calculation has been corrected for this fast drift component. For runs with  $|E| > 500$  V/cm the time step parameter itself must be reduced accordingly to avoid numerical errors underestimating the heating efficiency and the power deposited locally in the region of high electric fields.

I.3 Model of the electric field: The physical constraint is that the electric equipotential surfaces  $\psi = \text{const.}$  have to be identical with the magnetic flux surfaces  $\Psi = \text{const.}$  of the configuration used. Otherwise a poloidal field component  $E_\theta$  is generated which causes an unrealistic radial particle drift. For numerical reasons central ellipses are used in ODIN to fit the magnetic configuration computed from a Dommaschk field representation /5/. As seen from Fig. 1a this is a good approximation for  $r/a < 0.3$  only. But the position of the best fitted flux surface can be varied by the application of an additional vertical magnetic field  $0 < B_v < 50$  Gauss (Fig. 1b,c).

I.4 Error estimation for the code results: To estimate the errors induced by the electric field model, firstly the position of the best fitted magnetic surfaces was varied by varying  $B_v$  for parabolic potentials

$$\psi = \psi_a(r/r_a)^2 \quad \text{with } 1 \leq \psi_a \leq 7 \text{ kV.} \quad \text{In this way the}$$

erroneous poloidal field components  $E_\theta(r/a)$  introduced by the misfitting of the flux surfaces is changed in a wide range. In the worst case (i.e.  $B_v = 0$ ) the misfitting of the outermost flux surfaces is greatest where  $|E_\theta|$  reaches its maximum also resulting in the highest  $E_\theta$ -component there. It shows up (e.g. in Fig. 2 for 3.0 kV) that the code results are not sensitive to that variation indicating that  $|E_\theta(r/a)| < |E_{\theta, \text{crit}}(r/a)|$  in these cases,  $|E_{\theta, \text{crit}}|$  being the limit, where the erroneous field component starts to influence beam deposition. To get a number for  $|E_{\theta, \text{crit}}(r/a)|$  the elliptical equipotential surfaces were perturbed by changing their half axes  $\alpha \rightarrow \epsilon\alpha$ ,  $\beta \rightarrow \beta/\epsilon$  in order to generate an artificial poloidal component  $E_\theta(r/a)$ . Figure 3a shows the global results for different potentials  $\psi$ . Admitting an error of  $\pm 10\%$  for  $\eta$ , a critical field value  $|E_{\theta, \text{crit}}|$  can be deduced depending on  $\psi$ . The corresponding deposition profiles for 3.0 kV are plotted in Fig. 3b. Since the two methods should give consistent results one concludes that the code is not sensitive to  $E_\theta$ -components in the outer plasma region but to poloidal electric fields at  $r/a = 0.5$ . This is in accordance with the fact that this region is most frequented by the heating particles. In Fig. 5 the estimated critical poloidal field at  $r/a = 0.5$  is given as a function of  $\psi_a$  together with the value occurring in ODIN for the worst case (i.e.  $B_v = 0$ ). We conclude that the global and local ODIN results are correct within an error of 10% and 20%, respectively, if  $|E_\theta| < |E_{\theta, \text{crit}}|$  at  $r/a = 0.5$ , i.e.  $\psi_a < 5$  kV for a parabolic potential.

## II. Application of the revised code for WVII A

II.1 Heating efficiency: In Fig. 5a,b the recalculated  $\eta(\psi)$  for co resp. counter injection are given assuming parabolic potentials. The observed direction of the plasma rotation excludes negative  $\psi_a$  shown here for completeness. The experimental value  $\eta \approx 0.35$  for co and counter injection is very well represented by code results for  $\psi_a = (2.1 \pm 0.3)$  kV. This also holds for an electric field  $E(r) \propto \nabla\psi$  as seen from Fig. 5c.

II.2 Particle tracing method: The influence of the electric field on the ion orbits can be made visible by plotting the intersection points of the trajectories of a set of test particles with a given poloidal plane. The behaviour of the orbits for ions starting in the  $z = 0$  plane at different radii

R may be quantified by the area F(R) in the poloidal plane which surrounds these intersection points. In Fig. 6 an example for this confinement parameter F(R) for fast co-injected ions is shown. With increasing positive potential, the zone of good confinement, i.e. the minimum of F(R) is shifted towards the plasma center resulting in a more efficient trapping of the injected ions. For small negative potentials  $-1.0 \leq \Phi_a \leq -0.5$  kV no confinement is found corresponding to the poloidal drift resonance were the ExB-drift and the rotational transform drift for the fast ions cancel each other. Higher negative potentials would improve the confinement again beginning with ions starting at  $R < R_0$  caused by the counterwise poloidal rotation which then again is dominated by the electric field.

References

- /1/ W VII-A Team and Neutral Injection Team, Proc. 8th IAEA Conf. on Plasma Physics and Contr.Nucl. Fusion Research, Brussels 1980, Vol.I,p. 185
- /2/ W VII-A Team and Neutral Injection Team, Proc. 2nd Joint Grenoble-Varenna, Int. Symp. on Heating in Tor. Plasmas, 1980, Vol. II, p. 789
- /3/ W VII-A Team and Neutral Injection Team, Proc. 9th IAEA Conf. on Plasma Physics and Contr.Nucl. Fusion Research, Baltimore, 1982, Vol.II,p.241
- /4/ Maaßberg H., 1984, Proc. 5th Int.Workshop on Stellarators, Ringberg, FRG, Vol.II, P.507
- /5/ Dommaschk, W., 1978, IPP-Report 0/38.

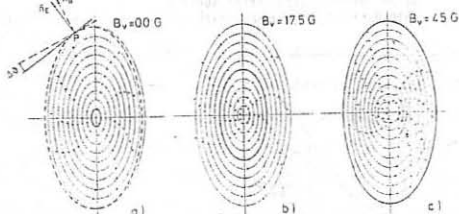


Fig.1: Equipotential surfaces used in ODIN for various vertical magnetic field components  $B_v$  plotted in the  $\theta = 18^\circ$  plane. The position of the best fitted flux surface is indicated by a fat line.  $\vec{n}_p$ : normal to the flux surface at a given point P  $\vec{E}_c$ : used direction for the electric field  $\vec{E}$  at this point.

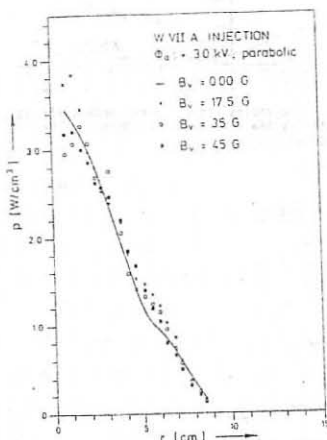
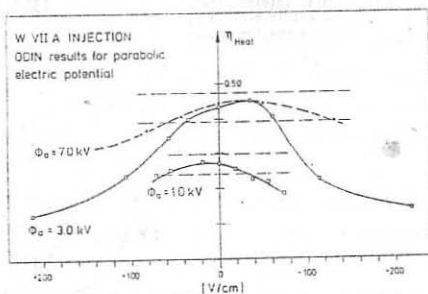


Fig.2: Power deposition profiles for different vertical magnetic fields  $B_v$ .



Maximum poloidal field component  $E_{g,max}$  for  $r/a=10$  ( $0 \leq \theta \leq 90^\circ$ )

Fig.3a: Heating efficiency as a function of  $E_{g,max}$  for perturbed equipotential surfaces

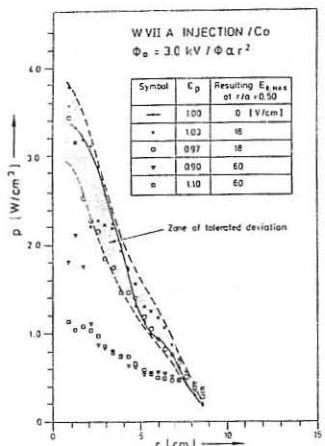


Fig.3b: Power deposition profiles for a set of perturbed equipotential surfaces with  $\theta_a = 3.0$  kV (parabolic)

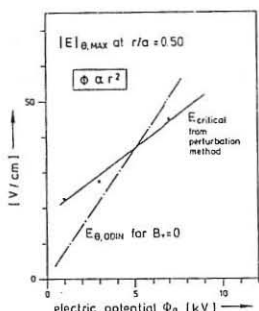


Fig.4: Critical poloidal field component as derived by the perturbation method

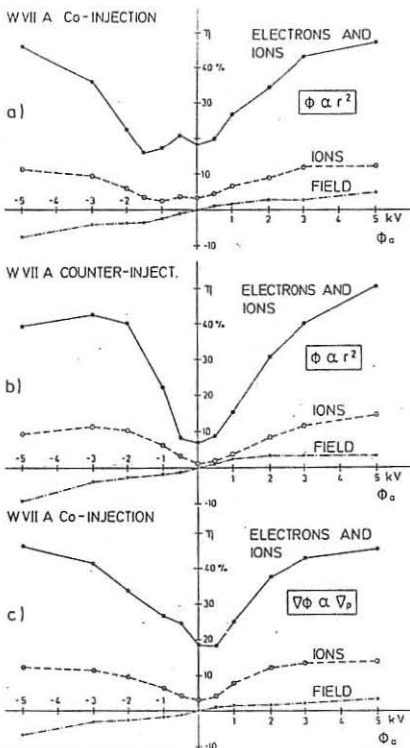


Fig.5: Heating efficiencies for different potentials as calculated by the new version of ODIN for shot Nr. 38000 at 180 ms

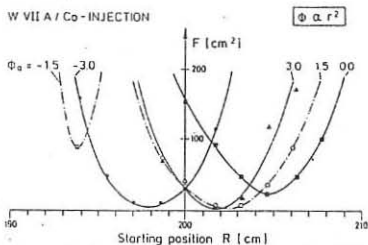


Fig.6: Variation of the confinement parameter  $F(R)$  with the strength  $\theta_a$  of a parabolic potential